

# CATION INTERDIFFUSION IN GaInP/GaAs SINGLE QUANTUM WELLS

Joseph Micallef, Andrea Brincat, and Wai-Chee Shiu\*

Department of Microelectronics, University of Malta, Msida MSD 06, Malta

\* Department of Mathematics, Hong Kong Baptist University, Waterloo Road, Hong Kong

## ABSTRACT

The effects of cation interdiffusion in  $\text{Ga}_{0.51}\text{In}_{0.49}\text{P}/\text{GaAs}$  single quantum wells are investigated using an error function distribution to model the compositional profile after interdiffusion. Two interdiffusion conditions are considered: cation only interdiffusion, and dominant cation interdiffusion. For both conditions the fundamental absorption edge exhibits a red shift with interdiffusion, with a large strain build up taking place in the early stages of interdiffusion. In the case of cation only interdiffusion, an abrupt carrier confinement profile is maintained even after significant interdiffusion, with a well width equal to that of the as-grown quantum well. When the interdiffusion takes place on two sublattices, but with the cation interdiffusion dominant, the red shift saturates and then decreases. The model results are consistent with reported experimental results. The effects of the interdiffusion-induced strain on the carrier confinement profile can be of interest for device applications in this material system.

## INTRODUCTION

The direct bandgap ternary semiconductor  $\text{Ga}_{0.51}\text{In}_{0.49}\text{P}$  lattice matched to GaAs has attracted much attention for a variety of electronic and optical applications including high-speed heterojunction bipolar transistors [1], field effect transistors [2], tandem solar cells [3], light emitting diodes [4], and infrared intrasubband photodetectors [5]. GaInP is a potential alternative to AlGaAs since it is not easily oxidised and does not suffer from a high concentration of deep trap centres.

Quantum well (QW) intermixing involves the interdiffusion of constituent atoms across the well-barrier interfaces, and is of particular interest since it offers the possibility of continuous, controlled modification of the material composition [6]. This change in composition alters the confinement profile and subband edge structure in the QW resulting in a modified effective bandgap of the QW structure. The extent of the intermixing, and thus of the modification of the subband edge structure, is a function of the QW intermixing technique parameters, such as the nature and concentration of the impurity species present, and the process temperature and time. Moreover the interdiffusion process can be localised to selected regions of the QW structure so that the optical properties of only the selected areas are modified by the interdiffusion process. QW intermixing can thus provide a useful tool for bandgap engineering.

Intermixing of lattice-matched AlGaAs/GaAs QW structures results in the interdiffusion of only group III atoms (Al, Ga) since there is no As concentration profile across the heterointerface. In contrast, the intermixing of lattice-matched  $\text{Ga}_{0.51}\text{In}_{0.49}\text{P}/\text{GaAs}$  QW structures can result in interdiffusion of both group III (Ga, In) and group V (P, As) atoms. Moreover, if the rates of interdiffusion on the two sublattices are not comparable, then a strained-layer

structure will result. Reported experimental results of thermal interdiffusion of lattice-matched GaInP/GaAs QWs have been interpreted in terms of substantial interdiffusion of the group III atoms together with minor interdiffusion of group V atoms [7]. Results of Si-impurity-induced intermixing have also been interpreted in terms of dominant group III interdiffusion [8].

## COMPUTATIONAL CONSIDERATIONS

An undoped GaAs single QW layer lattice-matched to  $\text{Ga}_{0.51}\text{In}_{0.49}\text{P}$  barriers is considered here. The constituent atoms compositional profile after interdiffusion is modeled using an error function distribution [9]. The interdiffusion of Ga and In atoms is characterized by a diffusion length  $L_d$ , which is defined as  $L_d = (Dt)^{1/2}$ , where  $D$  is the diffusion coefficient and  $t$  is the diffusion time; the interdiffusion of P and As atoms is characterized by a different diffusion length  $L'_d$ . For cation only interdiffusion  $L'_d = 0$ , while for dominant cation interdiffusion,  $L'_d \neq L_d$ , in both cases a strained QW structure results.

The QW structure will be coherently strained after interdiffusion if the layer thickness is within the critical thickness limit [10]. Tetragonal deformation results in a biaxial strain parallel to the interface and a uniaxial strain perpendicular to the interface. A compressive (tensile) biaxial strain causes an increase (decrease) in the bandgap energy whilst the uniaxial strain lifts the degeneracy of the heavy hole (HH) and light hole (LH) subbands, so that the HH subband moves towards (away from) the conduction band and the LH subband moves away from (towards) the conduction band. After interdiffusion, the well confinement profile, the carrier effective mass and the strain effects vary across the QW structure. Under these conditions, the subband-edge structure is obtained using the envelope function scheme by introducing these variations in the appropriate Schrödinger equation, which is then solved numerically to obtain the subband energy levels, the interband transition energies and the envelope wavefunctions. Details of the calculations are reported in [11].

## RESULTS AND DISCUSSION

The structure considered here is a 6 nm thick GaAs layer sandwiched between semi-infinite  $\text{Ga}_{0.51}\text{In}_{0.49}\text{P}$  barriers. Parameter  $k$  is defined as  $k = L'_d/L_d$ , and results are presented for  $0 \leq k < 1$ . A conduction band offset  $Q_c = 45\%$  [12] has been used in the calculations.

For  $k = 0$  interdiffusion takes place on the group III sublattice only. In this case a graded compositional profile results for the Ga and In atoms, while the P and As atoms compositional profile remains abrupt, as shown in Fig. 1(a) for  $L_d = 0.5$  nm. Ga diffuses into the barrier while In diffuses into the well forming an InGaAs/GaInP interface. Since the InGaAs lattice constant is always less than GaAs, the QW is under compressive strain, while a tensile strain arises in the barrier near the interface since the Ga concentration here is less than the lattice-matching composition of 0.51. The strain profile that is induced by the intermixing process is shown in Fig. 1(b). For  $L_z = 6$  nm and  $L_d = 0.5$  nm, no compressive strain results at the centre of the well, a 1.75% compressive strain in the well close to the interface, and a 1.75% tensile strain in the barrier close to the interface.

The abrupt change in the group V atoms compositional profiles produces an abrupt bandgap change at the interface from the InGaAs well to the GaInP barrier so that the carrier confinement profiles remain abrupt after interdiffusion, with a well width equal to that of the as-grown QW. The group III atoms graded compositional profile across the QW structure

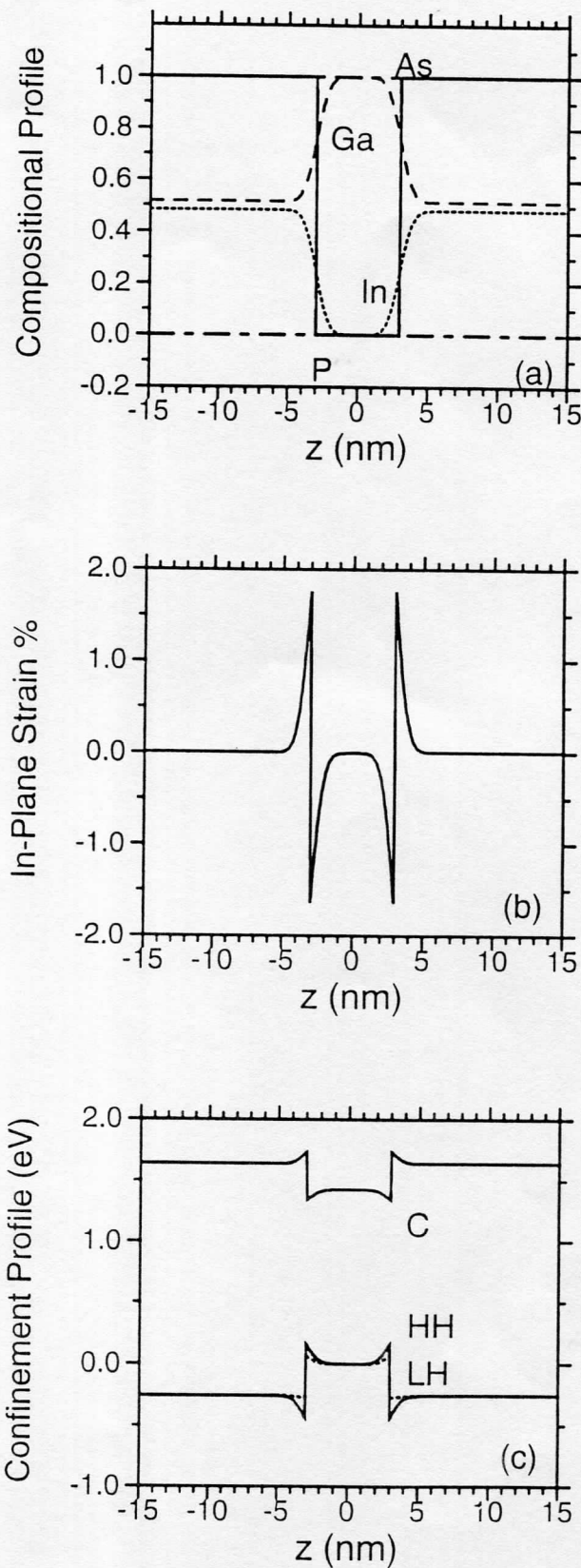


modifies the shape of the confinement profiles, while the effects of the strain distribution on this bandgap affects both the shape and separation of the conduction and valence bands, and the HH and LH potential wells no longer coincide, Fig. 1(c). In the well, the HH potential profile is shifted towards the electron (C) potential profile, while the LH potential profile is shifted away from the electron potential profile. In the barrier near the interface, the tensile strain again separates the HH and LH potential profiles, with the HH potential profile shifted away from, and the LH potential profile shifted towards, the electron potential profile. As a result of these strain effects, the C and HH confinement profiles exhibit a double well profile at the bottom of the well, and a double barrier structure similar to a resonant tunnelling structure. In the case of the LH confinement profile, the compositional and strain separation effects result in an almost square confinement profile after intermixing. Numerical results show that eigen states can be supported in the HH double-welled bottom potential, while tunnelling enhancement is possible for the topmost states in both the C and HH wells. The latter result could be of interest for intrasubband photodetector applications.

Fig. 1(a). Composition profile for  $L_z = 6$  nm,  $L_d = 0.5$  nm, with well centre at  $z = 0$ .

Fig. 1(b). In-plane strain for the interdiffused QW

Fig. 1(c). Carrier confinement profiles for electron (C), heavy hole (HH) and light hole (LH), showing double-well feature at the well bottom.



The variation of strain inside the well with interdiffusion is shown in Fig. 2(a). In the initial stages of interdiffusion ( $L_d \leq 0.5$  nm for the QW under consideration) a large compressive strain builds up in the well near the interface, while the centre of the well is still practically unstrained since the compositional change at the centre is still minimal. As interdiffusion proceeds In atoms diffuse to the centre of the well so that the group III atoms composition in the centre of the well starts to change and the well centre becomes compressively strained. For longer interdiffusion,  $L_d = 4$  nm, the strain profile across the QW becomes fairly uniform, mirroring the compositional distribution. The tensile strain in the barrier near the interface remains practically the same as interdiffusion proceeds, Fig. 2(b).

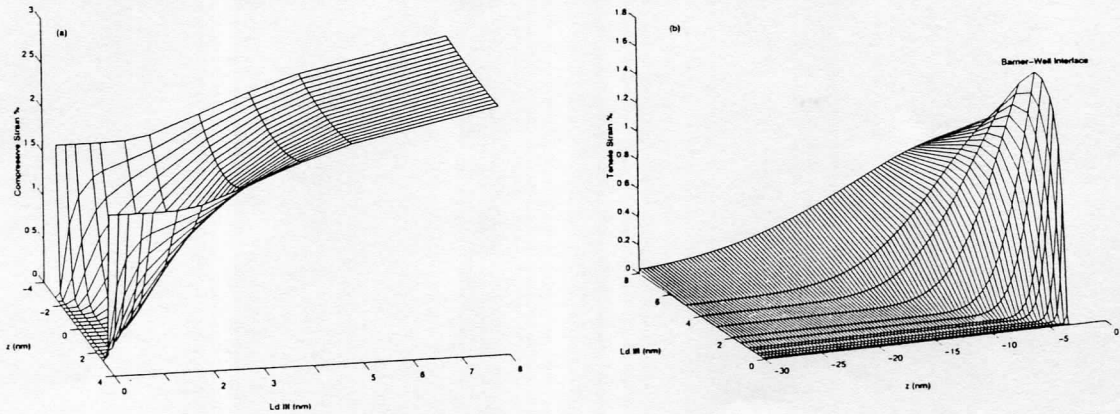


Fig. 2. (a) Compressive strain distribution across the QW with variation in interdiffusion; (b) tensile strain distribution in the barrier near the well interface with variation in interdiffusion. Group III atoms only interdiffusion.

The ground state electron-HH (C1-HH1) and electron-LH (C1-LH1) transition energy change with  $L_d$  are shown in Fig. 3. The effective QW bandgap energy of the intermixed structure is the C1-HH1 transition, and in this case the HH1 state occurs in the double-well potential, for small values of  $L_d$ . As the interdiffusion proceeds the bandgap energy decreases, corresponding to a shift to longer wavelengths, as evidenced in experimental results [7]. The shift to longer wavelengths with interdiffusion is similar to experimental results for Zn-diffusion induced intermixing of  $\text{In}_{0.53}\text{Ga}_{0.47}\text{As}/\text{InP}$  QWs. In contrast, interdiffusion in  $\text{AlGaAs}/\text{GaAs}$  [9] and  $\text{InGaAs}/\text{GaAs}$  [13] QW structures, as well as  $\text{InGaAs}/\text{InP}$  induced by sulphur diffusion [14], results in bandedge shifts to shorter wavelengths.

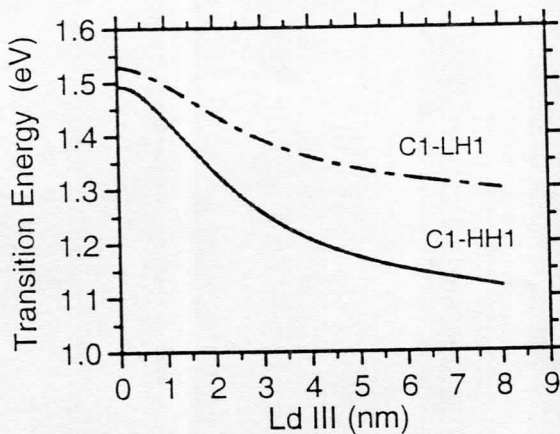


Fig. 3. Heavy-hole and light-hole ground state transition energy variation with  $L_d$  for group III atoms only interdiffusion.

For  $0 < k < 1$ , interdiffusion takes place predominantly on the group III sublattice, along with minor interdiffusion on the group V sublattice. Strain is again induced in the intermixed QW structure since  $L_d' \neq L_d$ , having a similar profile as for  $k = 0$ , with compressive strain in the well and tensile strain in the barrier close to the interface. For the case  $k = 0.25$ ,  $L_z = 6$  nm, and  $L_d = 0.5$  nm, the strain at the well centre, in the well close to the interface, and in the barrier close to the interface, shows a decrease of about 40%, Fig. 4(a). Since interdiffusion now takes place on the two sublattices the carrier confinement profiles are no longer abrupt, while the double-well potential at the well bottom and the double barrier profile at the top of the well are much less pronounced, as shown in Fig. 4(b).

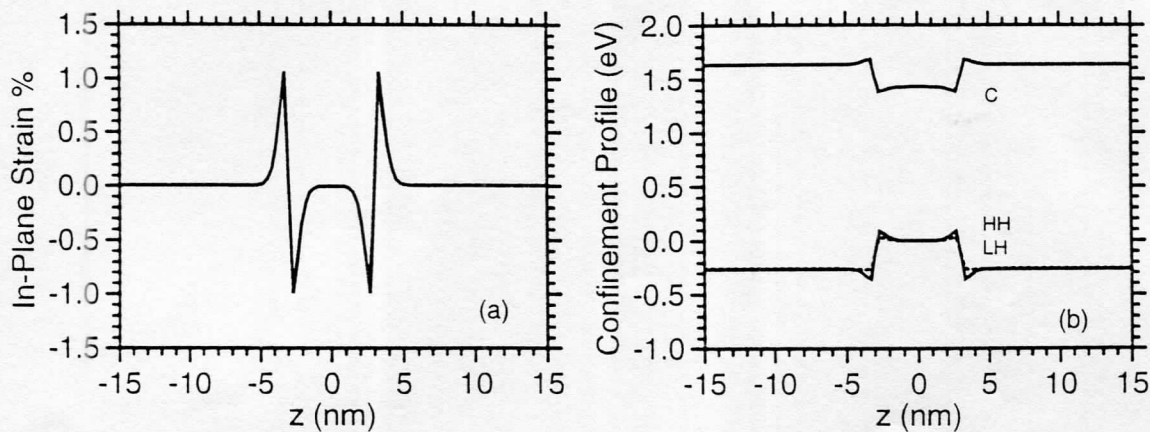


Fig.4. (a) In-plane strain and (b) carrier confinement profiles, for the interdiffused QW with  $L_z = 6$  nm,  $L_d = 0.5$  nm,  $k = 0.25$ .

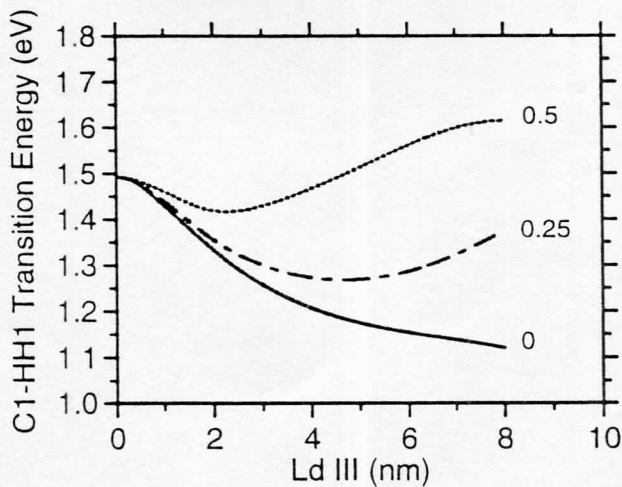


Fig. 5. Ground state transition energy shift with interdiffusion for different values of  $k = L_d' / L_d$ .

The variation of the ground state transition energy with interdiffusion, for different values of  $k$ , is shown in Fig. 5. The QW bandgap energy is the C1–HH1 transition, reflecting the compressive nature of the strain induced in the QW by the intermixing process. As already noted the bandgap energy decreases for  $k = 0$  as the interdiffusion proceeds, corresponding to a large red shift of the effective bandgap of the interdiffused QW. When  $k = 0.25$ , a red shift in the effective bandgap again results. However, for long enough interdiffusion duration, the red shift saturates and even decreases. The results obtained from our model correspond to experimental results reported for disordering of  $\text{Ga}_{0.51}\text{In}_{0.49}\text{P}/\text{GaAs}$  QWs by thermal annealing [7], showing the



red shift saturating and decreasing with increasing duration of the QW disordering process. For  $k = 0.5$ , the red shift again saturates and then decreases, but at an earlier stage of the interdiffusion process, since the competing group V sublattice interdiffusion is now more pronounced. Thus for  $k < 1$ , the ground state transition energy variation (saturation and subsequent decrease of the red shift) provides an indication of how dominant the group III atoms interdiffusion is with respect to the group V interdiffusion.

## CONCLUSIONS

QW intermixing of  $\text{Ga}_{0.51}\text{In}_{0.49}\text{P}/\text{GaAs}$  single wells has been modeled for cation only interdiffusion, and for dominant cation interdiffusion. Strain build up results in both cases and this is included in the model. In the case of cation only interdiffusion an abrupt confinement profile is maintained even after significant intermixing, with the confinement profile exhibiting a double-well potential profile at the bottom of the well. For both cases a red shift is evidenced after interdiffusion. This red shift saturates and then decreases when minor anion interdiffusion is also present. The model results compare well with reported experimental results.

## ACKNOWLEDGEMENT

This work was supported in part by the RGC Earmarked Research Grant of Hong Kong.

## REFERENCES

- 1 J.-I. Song, C. Caneau, K.-B. Chough, and W. P. Hong, IEEE Electron Device Lett. **15**, 10 (1994).
- 2 M. Razeghi, F. Omnes, M. Defour, P. Maurel, P. Bove, Y.J. Chan, and D. Pavlidis, Semicon. Sci. Technol. **5**, 274 (1990).
- 3 T. Takamoto, E. Ikeda, H. Kurita, and M. Ohmori, Appl. Phys. Lett. **70**, 381 (1997).
- 4 K. Koyabashi, S. Kawata, A. Gomyo, I. Hino, and T. Suzuki, Electron. Lett. **21**, 931 (1985).
- 5 C. Jelen, S. Slivken, J. Hoff, M. Razeghi, and G.J. Brown, Appl. Phys. Lett. **70**, 360 (1997).
- 6 M.D. Camras, N. Holonyak, Jr., R.D. Burnham, W. Streifer, D.R. Scifres, T.L. Paoli, and C. Lindström, J. Appl. Phys. **54**, 5637 (1983).
- 7 C. Francis, M.A. Bradley, P. Boucaud, F.H. Julien, and M. Razeghi, Appl. Phys. Lett. **62**, 178 (1993).
- 8 R.L. Thornton, F.A. Ponce, G.B. Anderson, and F.J. Endicott, Appl. Phys. Lett. **62**, 2060 (1993).
- 9 T.E. Schlesinger and T. Kuech, Appl. Phys. Lett. **49**, 519 (1986).
- 10 R.L. Thornton, D.P. Bour, D. Trent, F.A. Ponce, S.C. Tramontana, and F.J. Endicott, Appl. Phys. Lett. **65**, 2696 (1994).
- 11 J. Micallef, E.H. Li, and B.L. Weiss, J. Appl. Phys. **73**, 7524 (1993).
- 12 S.D. Gunapala, B.F. Levine, R.A. Logan, T. Tanbun-Ek, and D.A. Humphrey, Appl. Phys. Lett. **57**, 1802 (1990).
- 13 G.P. Khotiyal and P. Bhattacharya, J. Appl. Phys. **63**, 2760 (1988).
- 14 I.J. Pape, P. Li Kam Wa, J.P.R. David, P.A. Claxton, and P.N. Robson, Electron. Lett. **24**, 1217 (1988).